Design and Implementation of a Rotorless Wind Turbine Simulator

Kecan Yu
Electrical & Computer Eng.
Illinois Institute of Tech. (IIT)
Chicago, IL, USA
kyu17@hawk.iit.edu

Kevin Norman, Shafquat Yasar Aurko, Beibei Ren
Mechanical Engineering
Texas Tech University
Lubbock, USA
{kevin.b.norman, saurko, beibei.ren}@ttu.edu

Qing-Chang Zhong
Electrical Engineering
SYNDEM LLC and IIT
Chicago, IL, USA
zhongqc@ieee.org

IECON 2024 - 50th Annual Conference of the IEEE Industrial Electronics Society | 978-1-6654-6454-3/24/$31.00 ©2024 IEEE | DOI: 10.1109/IECON55916.2024.10905783

***Abstract*—Wind turbine simulators (WTS) play a crucial role in laboratory training and research on wind power systems. Existing simulators often use physical components like motors and permanent magnet synchronous generators (PMSG), which are bulky and heavy. This paper proposes a rotorless WTS featuring a digitally embedded mathematical model and a power electronic converter that emulates a wind power generator. The mathematical model integrates the models of a wind turbine, a gearbox, and a PMSG, and the power electronic converter produces a single-phase AC output. The system features an AC-DC-AC converter arranged in the θ-converter topology with a rectification leg, a neutral leg and an inversion leg, eliminating the need for external DC sources or isolation transformers. Independent controllers for the rectification, neutral, and inversion legs are proposed to ensure multiple objectives are met at the same time. Simulation and experimental results are presented to demonstrate the feasibility and effectiveness in replicating a physical wind turbine-PMSG system.**

***Index Terms*—Wind Turbine Simulator, PMSG, SYNDEM Smart Grid Research and Educational Kit, θ-converter.**

I. Introduction

Wind power generation systems (WPGS) stand as prominent contributors to the renewable energy sources (RES) and decentralized power generation initiatives. To facilitate the seamless integration of WPGS into the evolving smart grid, adequate testing, training, and research within laboratory settings are imperative. Nonetheless, operating a WPGS within a laboratory environment is challenging as conventional wind turbines (WT) have long blade spans and large gearboxes, and the generators paired with them are also bulky. Wind Turbine Simulators (WTS) can alleviate such challenges by emulating the behavior of WT within the confines of a relatively small hardware setup, making them ideal for learning and research in laboratory settings. Simulators enable reliable and reproducible indoor testing and data collection, while also providing a training opportunity for students and researchers [1].

The WTS acts as a power source, which can provide varying power output in accordance with the wind profile provided. The WTS consists of the aerodynamic properties of a WT and the dynamics of a PMSG. The varying wind characteristics are set as the input for the mathematical model, which then enables the digital signal processing (DSP) unit to generate the equivalent excitation current and voltage at the generator. However, a prevalent hardware setup across most literature involves a physical motor-generator pair to produce equivalent voltage and current profiles. In certain studies such as [2]–[5], a DSP model processes the wind profile and generates reference voltage and current signals. These signals drive a DC motor drive, which in turn generates torque to operate a permanent magnet synchronous generator (PMSG) for supplying the load. This set-up presents several limitations, which includes the necessity for a greater space constraint, particularly when a DC motor is utilized. Moreover, the presence of moving parts increases the risk of failure, cost, and limits scalability. [6] proposes an electronic WTS which does not utilize a physical motor-generator pair. While this is an improvement over the physical motor-generator set, it uses two separate modules for the rectification and inversion.

This paper introduces a WTS capable of accurately emulating a WPGS without the need for physical motors and generators, with the power electronic systems all included within a single compact module. The system's mathematical model incorporates a WT and gearbox emulator capable of generating torque supplied to a PMSG model [7], all embedded within the DSP. The PMSG model produces the reference voltage used to control the IGBT legs of an inverter, to generate the appropriate voltage and frequency at the output. The SYNDEM Smart Grid Research and Educational Kit (hereafter referred to as "the Kit") [8] is used in this application, which is a reconfigurable power electronics converter, to process the reference signals received from the DSP and supply the load at the output. This setup ensures that experiments can be conducted in a laboratory setting without the need for long blades, complicated gearboxes or heavy PMSGs. The main contributions of this work are:

- Formulation and implementation of a comprehensive WPGS model that integrates the dynamics and characteristics of a WT, gearbox, and PMSG within an all-in-one structure. Unlike conventional WPGS setups, which use separate physical components, this model consolidates these elements into a streamlined, discretized form embedded in the DSP of the power converter. Consequently, the device generates a sinusoidal voltage, with amplitude and frequency directly correlating to real-time variations in wind speed and blade length. These parameters can

be adjusted by users via a user-friendly human machine interface (HMI). The single-phase output helps to reduce the overall component count, simplifies the structure of the power circuit, and streamlines installations into systems such as microgrids.

- The control framework tailored for an AC-DC-AC converter that adopts the θ-converter [9] topology, consolidating the simulator within a single device structure. This ensures that unlike the WTS that use physical DC motors, the proposed WTS does not require any separate DC source. This control is designed to manage three power legs: the rectification, neutral, and inversion legs. The rectification leg utilizes a self-synchronized universal droop control (SUDC) [10], tailored for the θ-converter, along with resonant compensators and power control features [11]. The neutral leg employs a proportional integral (PI) control with a resonant compensator. These features aim to achieve unity power factor, regulate power exchanged from the grid, rectify the AC input, and stabilize the DC bus voltage. The inversion leg control emulates the output signal of the mathematical model, mimicking a WT output.

The proposed system is demonstrated experimentally, featuring an interface with a customized HMI that interacts with the power electronics device for real-time control and monitoring.

II. Overview of a WTS

The proposed WTS is implemented on the Kit's power board and the system can support multiple external load types, such as resistive, capacitive or inductive. It can also be connected with external switched mode power supplies, such as the maximum power point tracking converters, to achieve the maximum power output in variable input conditions. The proposed simulator emulates variable speed WPGS, as these have a higher energy yield in comparison to fixed-speed ones [12]. With the overall setup depicted in Figure 2, a WTS comprises four main parts: the mathematical model (components shown in Figure 1), the controller, the power conversion stage (PCS), and the HMI.

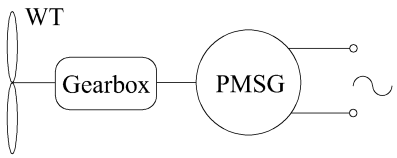

Fig. 1. Illustrative Wind Power Generation System with PMSG

1) Mathematical Model: Embedded into the DSP of the platform. The main objective is to mimic the behavior and dynamics of a WPGS. It consists of three sub-models: a WT, gearbox, and PMSG.
   a) WT model: Processes the wind speed (V_W) and blade length (R) input which are set by the user from the HMI. R, V_W and the rotor speed ω_R are used to calculate the tip-speed ratio λ. This in turn is used to calculate the power coefficient (c_p) which generates the rotor torque (T_R) of the turbine.
   b) Gearbox model: Increases the rotor speed of the WT to a higher speed suitable for driving the generator, thereby propagating the mechanical energy captured by the WT model into the PMSG model. It converts T_R from the WT model to the mechanical torque (T_m), which is transmitted to the PMSG model. It also takes in the rotor speed of the PMSG model (ω_m) and transmits it to the WT model by converting it to ω_R.
   c) PMSG Model: Takes the T_m input from the gearbox and generates a single-phase output voltage with the appropriate voltage amplitude and frequency. It also calculates the mechanical speed ω_m from the electrical speed ω as $\omega = p\omega_m$ with p being the the number of pairs of poles of the PMSG magnets and feeds this back in the gearbox, which then goes to the WT model.
2) Controller: Comprises of a set of algorithms responsible for monitoring and adjusting multiple objectives. Implemented within the DSP of the simulator, these controllers modulate the IGBT gates of the power board to achieve goals such as tracking the reference signals generated by the mathematical model. An effective controller is characterized by a rapid response in reference tracking, stable steady-state operation, adaptability to disturbances, and decoupled control for the multiple power stages.
3) PCS: Translates the power generation signals generated by the mathematical model into physical power signals. Utilizing a power electronic unit configured as a single-phase AC-DC-AC converter, the PCS generates the expected AC voltage output at the load to mimic the behavior of a WPGS. The topology used here takes single-phase AC electricity from the utility grid, rectifies it, and then converts it to a single-phase AC output.
4) HMI: Serves as the visual user interface where the wind profile and the WT parameters can be changed in real-time. The HMI allows users to program parameters such as V_W, so that a realistic outdoor condition can be developed. R can be selected in accordance with the power requirements and scale of the WT which the user wants to mimic. The HMI also allows for real-time visualization of signals, which are transmitted by the on-board sensors of the power converter. This is achieved by using RS485 serial communication protocols and MATLAB/Simulink as the front-end software, further allowing for post-processing plots and tools [1].

III. Design and Implementation of a WTS

The proposed system design integrates all components of the WTS, as illustrated in Figure 2, into a single device – the SYNDEM Kit. This Kit, characterized as a reconfigurable, open-source power electronic converter, consolidates a control and power board into a single unit. The Kit empowers users

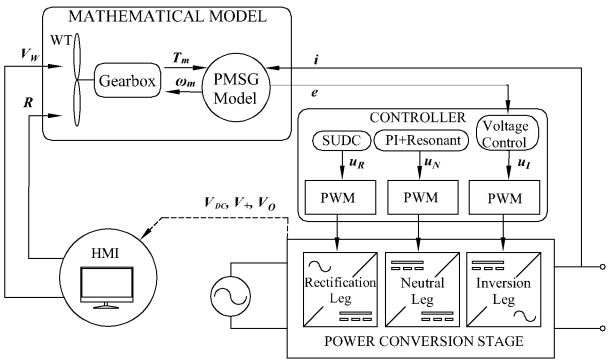

Fig. 2. Structure of the Proposed Wind Turbine Simulator

to directly integrate the proposed mathematical model and control algorithms into its DSP, thus providing configuration flexibility. Moreover, the Kit effectively emulates the power transmission behavior of a WT model through its reconfigurable power board, set as an AC-DC-AC converter, commonly referred to as a back-to-back converter. A key feature of this Kit is its automatic code generation, utilizing the TI C2000 control card as its DSP and ensuring compatibility with TI Code Composer Studio. This integration simplifies the use of MATLAB/Simulink's graphical programming environment, making it easier to implement mathematical models and control algorithms.

Figure 2 illustrates the overall system structure. The user provides V_W and R using the HMI. This is then processed by the mathematical model– first by the WT model, followed by the gearbox model and then the PMSG model, which also takes the inductor current feedback (i) from the output terminal as an input. The PCS utilizes three legs: the neutral, rectification, and inversion legs, each controlled by a set of independently controlled algorithms. The rectification and neutral legs, which are controlled by the control signals u_R and u_N respectively, convert the AC utility input into DC electricity, which serves as the power supplyto the inversion leg. The inversion leg tracks the reference signal from the mathematical model (e) to generate a single-phase AC output, by using a voltage controller with control signal u_I. The sensors on the Kit measure the DC bus voltage (V_{DC}), the inverter input voltage (V_+) and the output terminal voltage (v_o). Detailed descriptions of the mathematical model, PCS, and controllers are provided in the subsequent subsections.

A. Mathematical Model Implementation

As illustrated in the top-left part of Figure 2, the mathematical model comprises the WT model, the gearbox model, and the PMSG model, all chained together.

1) Wind Turbine Model: In a physical WT, the wind pushes the blades of the turbine and causes a mechanical torque to be generated. The same process is replicated in the WT model. Thereference signals V_W and R are sent through the HMI into the DSP to generate the virtual mechanical power (mechanical torque $\times$ rotation speed), which can be calculated as

$$P_m = \frac{1}{2}\rho\pi R^2 V_W^3 c_p(\lambda,\beta), \tag{1}$$

where P_m is the mechanical output power (W), ρ is the air density (kg/m^3), c_p is the power coefficient that denotes the aerodynamic efficiency of a WT and depends on the tip speed ratio λ of the WT and the angle of blades β (°). The $c_p$can be modeled with a mathematical function of λ and β. Here, the method in [13] is adapted to model c_p as

$$c_p(\lambda,\beta) = 0.22(\frac{116}{\beta} - 0.4 - 5)e^{\frac{-12.5}{\beta}}, \tag{2}$$

with

$$\beta = \frac{1}{\frac{1}{18\lambda+1.44\lambda} - \frac{0.035}{(18\lambda)^3+1}}. \tag{3}$$

The tip-speed ratio λ, which is the ratio between tangential speed of the turbine rotor and wind speed, is defined as

$$\lambda = \frac{\omega_R R}{V_W}, \tag{4}$$

for which, the optimal tip speed ratio λ_{opt} is 0.4 and the maximum c_p is 0.42. The rotor torque of the turbine T_R is calculated by dividing P_m by ω_R, and is then transmitted to the gearbox model.

2) Gearbox Model: With the gearbox ratio n, the gearbox scales up the speed to match with the mechanical speed of the generator

$$\omega_m = n\omega_R \tag{5}$$

and reduces the rotor torque T_R from the WT model to the mechanical torque for the PMSG as

$$T_m = \frac{1}{n}T_R. \tag{6}$$

3) PMSG Model: This model emulates a PMSG, as described in [7]. Assuming that the resistance of the stator winding is R_s, the summation of self inductance and mutual inductance of the PMSG is L and the stator phase current is i, the phase terminal voltage v is

$$v = -R_s i - L\frac{di}{dt} + e, \tag{7}$$

where e is the voltage generated by the PMSG as

$$e = K_m\dot{\theta}\sin\theta, \tag{8}$$

where θ is the phase of the output voltage, $\dot{\theta} = \omega$ is the electrical speed, and K_m is the machine constant of the PMSG. While the electrical part of the PMSG model generates the output phase voltage as shown above, there is also a need to model the mechanical part of the PMSG through

$$J\ddot{\theta} = T_m - T_e - D_p\dot{\theta}, \tag{9}$$

where J is the moment of inertia of all rotating parts connected to the rotor, D_p is the damping factor, T_m is the mechanical torque, and T_e is the electromagnetic torque given by

$$T_e = K_m i\sin\theta. \tag{10}$$

B. Power Conversion Stage (PCS)

The WTS comprises three power legs: rectification, neutral, and inversion. The topology, as depicted in Figure 3, consists of six IGBT switches, five capacitors, and three inductors. Notably, this structure enables independent control for each leg, with each driven by a pair of complementary IGBTs, providing flexibility for the controllers to achieve different objectives. The single-phase rectifier converts an AC input from the utility grid. The common AC neutral and DC negative terminal feature of the θ-converter topology reduces common mode currents, eliminates the requirement for an isolation transformer, utilizes only four switches, and introduces two independently controlled legs – rectification and neutral. The rectification leg includes switches Q_1 and Q_2, an inductor L_1, and a DC bus capacitor C_{77}, with voltage denoted as V_{DC}. This leg acts as a half-bridge rectifier that regulates the DC bus voltage V_{DC}. The neutral leg consists of switches Q_3 and Q_4, an inductor L_2, and capacitors $C_{78}+C_{76}$, with voltage across denoted as V_+. The neutral leg acts as a DC-DC converter and is responsible for regulating the voltage V_+ which sets a stable reference point for the subsequent inversion leg. The inversion leg is utilized to convert the DC electricity into a single-phase AC and consists of switches Q_5 and Q_6, along with an LC filter composed of inductor L_3 and capacitor C_{80} on the output side.

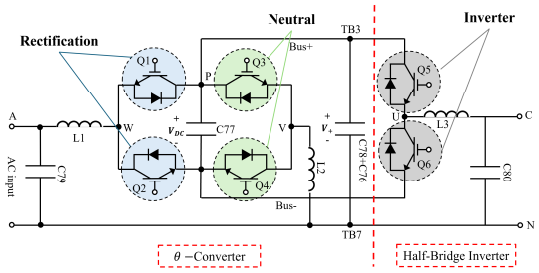

Fig. 3. AC-DC-AC Converter Using θ-Converter

C. Control of Rectification Leg

The rectification leg primarily focuses on regulating the grid current to achieve unity power factor, regulates the power exchanged with the grid at the input side, and also serves as a half-bridge rectifier that regulates V_{DC} to a reference value V_{DC}^*. The control mechanism for the rectification leg employs a SUDC [10] along with power regulation techniques [11], augmented with additional modifications. Figure 4 depicts the control structure of the rectification leg. In this setup, V_{DC} is maintained by setting the reference power set-mode to P_{set} for the SUDC to operate, where v_g and i_g represent the voltage and current of the grid, respectively. v_{DC} denotes the DC bus voltage after passing through a low pass filter (LPF) to remove high-frequency components, P_{out} represents the output power generated at the output side of the simulator, and $K_{R1}(s)$ is a resonant compensator added to the SUDC to eliminate second and third harmonics ($h = 2, 3$) of the grid fundamental frequency. The resonant compensator $K_{R1}(s)$ is defined as

$$K_{R1}(s) = \sum_{h=2,3} \frac{2K_h \zeta h\omega_g s}{s^2 + 2\zeta h\omega_g s + (h\omega_g)^2}, \tag{11}$$

with K_h being the harmonic gain that can be defined experimentally, $\zeta = 0.01$ being the damping factor , and $\omega_g = 2\pi f$ with f being the fundamental frequency of the grid [1]. Finally, the controller sends a control signal u_R, which undergoes scaling factors to define the duty cycles, as detailed in [9]. These duty cycles then regulate switches Q_1 and Q_2, setting the stage for the subsequent legs.

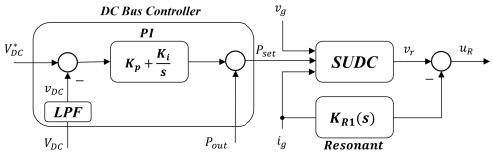

Fig. 4. Rectification-leg Controller

D. Control of Neutral Leg

The neutral leg functions as a DC-DC converter, with the aim of maintaining the voltage V_+ at its reference value V_+^*. This is achieved through the implementation of a PI controller, complemented by a resonant filter to divert second and third harmonic components of the grid fundamental frequency from V_+. The resonant filter is denoted as $K_{R2}(s)$ and takes the same form as $K_{R1}(s)$, but with different K_h values. Then, the control output u_N undergoes scaling before being converted into PWM signals, which in turn drive switches Q_3 and Q_4, as depicted in Figure 5.

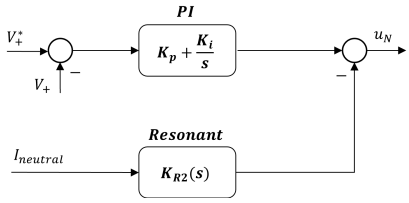

Fig. 5. Neutral-leg Controller

E. Control of Inversion Leg

Once control of the rectification leg and the neutral leg is established, the inversion leg can beactivated. The inversion leg reproduces the voltage e generated by the PMSG model at the output of the PCS. In this paper, for the sake of simplicity, an open-loop controller is adopted.

F. HMI

The user interface, configured within MATLAB/Simulink, facilitates data transmission and reception via a serial interface utilizing RS485 communication at a sampling rate of 1 ms. This interface allows users to adjust parameters such as V_W and R, as depicted in Figure 6. This flexibility arises from the digital integration of the WT model, which employs direct

calculations derived from Subsection III-A. When modifying turbine parameters, such as V_W and R, T_m changes, leading to a corresponding change in T_e, thereby affecting the frequency and magnitude of the output voltage. Users can monitor signals such as c_p, P_m, P_{out}, V_O, $\dot{\theta}$, V_{DC}, V_+, among others, in a user-friendly display. Furthermore, these signals can undergo further analysis and post-processing in MATLAB.

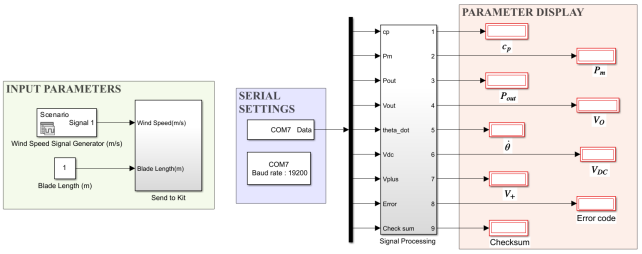

Fig. 6. HMI of the WTS

IV. Simulation Results

A. Simulation at Rated Parameters

In this paper, the simulation is implemented using the MATLAB/Simulink Toolbox. The maximum step size for the simulation is set to 1×10^{-6} seconds, and the sample time is specified as 3/20000 seconds, aligning with the sample time used in the TI C2000 Controlcard. The model simulates a small WT, with a blade length of 1 m. The pitch angle β is taken as 0°. The air density is taken as 1.225 kg/m^3, which is the standard atmospheric pressure at sea-level. The moment of inertia J is 1.4×10^{-6} kgm^2, the damping factor D_p is 3.37×10^{-4} and the machine constant K_m is 0.1326. The number p of pairs of poles is 4 and the gearbox ratio n is selected as 60. For the simulation, the wind speed is selected as 7 m/s.

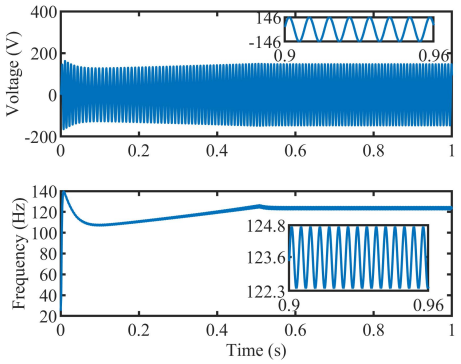

Fig. 7. Simulation Result: Voltage and Frequency

Figure 7 displays the output wave-forms that have been observed from the simulation. The frequency of the WT, which is utilized within the WT model, has been observed to be approximately 123.6 Hz, which is then used to generate the voltage reference value within the PMSG model, and is then transmitted to the power converter. The voltage output from the inversion leg reaches the steady state at 0.7 seconds. The output is observed to be a clean sinusoidal waveform with the RMS voltage of 103.2 V.

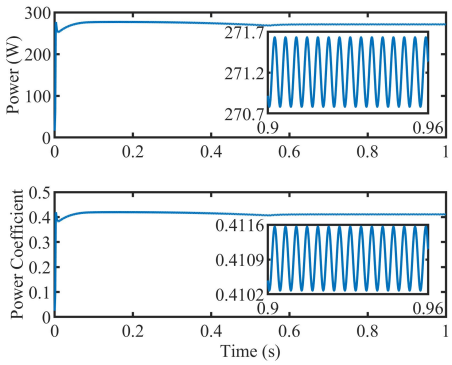

Fig. 8. Simulation Result: Power Curve

Figure 8 displays the waveforms of P_m and c_p. The WT model generates mechanical power of 271.2 W. c_p is 0.4109, which depends on the load chosen as 50 Ω. The curve illustrates that the power generated by the WTS is directly proportional to c_p, consistent with the working principle of standard WTS.

V. Experimental Results

After the successful implementation of the WT model in Simulink, an experimental assessment was conducted to validate the proposed WTS for practical application. Figure 9 illustrates the experimental setup, all within a single device– the SYNDEM Kit, rendering the setup compact and portable. The only additional hardware components required for this experiment include a computer, which hosts the HMI, an RS485 module used to transmit/receive data, and a resistive load connected at the output terminals. The Kit comprises of fixed components with reconfigurability capabilities, utilizing the component values detailed in Table I. The platform also incorporates built-in protection features to safeguard against values exceeding their rated operational conditions.

Fig. 9. Experimental Setup

The input parameters used in the experimental setup were identical to those utilized in the simulation. Initially, the experiment was conducted with a 50 Ω load. Figure 10 illustrates the output voltage v_o and current i at the output terminal of

TABLE I
POWER BOARD PARAMETERS

Components		Values
Input Capacitor	C_{79}	$20\mu F$
DC Bus Capacitor (V_{DC})	C_{77}	$470\mu F$
Neutral Leg Capacitor (V_+)	C_{78}, C_{76}	$20\mu F, 470\mu F$
AC Output Capacitor	C_{80}	$20\mu F$
Input, Neutral, AC Output Inductors	$L_{1,2,3}$	$1.5mH$

the Kit, as well as the input grid current i_g and V_{DC}. Channel 1 displays the output voltage, approximately 94.6 V RMS at a frequency of 132.1 Hz, generated by the inversion leg. The output current is shown on Channel 2, with an RMS value of 2.51 A. Channel 3 shows the voltage V_{DC}, which is controlled to steadily hover around the reference 400 V. Finally, Channel 4 shows the grid input current at around 60 Hz, different from the frequency of the output. The experimental test successfully demonstrates the operation of the WTS, offering a valuable tool and potential for exploration in WPGS.

In the conducted study, discrepancies between the simulation and experimental results were observed, particularly in voltage frequency and power measurement. The simulation predicted a frequency of 123.6 Hz with an RMS Voltage of 103.2 V. The experimental results indicated a moderately higher frequency of 132.1 Hz with a slightly lower RMS voltage of 94.6 V. These variations can be attributed to several factors, such as measurement errors and inaccurate component parameters, which are expected to be rectified after adopting a closed-loop controller for the inversion leg.

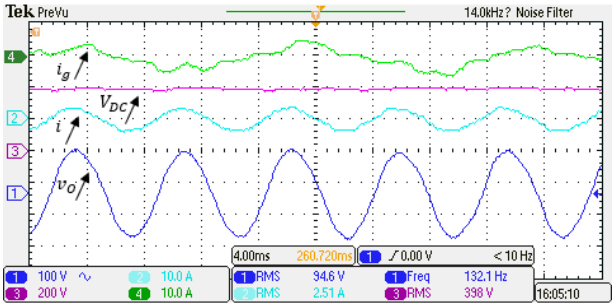

Fig. 10. Experimental Results with 50 Ω Load

VI. CONCLUSION

WTS plays a vital role in facilitating training and research on WPGS. The all-in-one rotorlessWTS proposed in this paper is anticipated to deliver high performance while offering flexibility, as it consolidates the entire hardware setup into a single compact device. This study establishes the mathematical model of the proposed WTS, capable of generating single-phase AC output power directly proportional to that produced by a physical PMSG driven by a WT. The control framework is built upon the θ-converter, which has advantages such as reducing component count and streamlining system integration. Simulation results validate the accuracy of the mathematical model in producing a reference voltage corresponding to the wind profile. Experimental analysis conducted on the SYNDEM Kit further confirms the effectiveness of the proposed system, generating the proper output voltage at the output terminal. Both simulation and experimental results have demonstrated the feasibility and performance of the proposed WTS system. Although the simulations are carried out with a single-phase output, it can be easily changed to produce three-phase outputs.

ACKNOWLEDGMENT

This work was supported in part by the National Science Foundation under Grant #2328248 and #1810105.

REFERENCES

[1] K. Norman, B. Ren, and Q.-C. Zhong, "Learning-by-doing: Design and implementation of a solar array simulator with a SYNDEM smart grid research and educational kit," *IEEE Power Electronics Magazine*, vol. 11, no. 1, pp. 47–54, Mar. 2024.

[2] M. E. Abdallah, O. M. Arafa, A. Shaltot, and G. A. A. Aziz, "Wind turbine emulation using permanent magnet synchronous motor," *Journal of Electrical Systems and Information Technology*, vol. 5, no. 2, pp. 121–134, Sep. 2018.

[3] A. Hazzab, H. Gouabi, M. Habbab, M. Rezkallah, H. Ibrahim, and A. Chandra, "Wind turbine emulator control improvement using nonlinear PI controller for wind energy conversion system: Design and real-time implementation," *International Journal of Adaptive Control and Signal Processing*, vol. 37, no. 5, pp. 1151–1165, Feb. 2023.

[4] Y. Sirouni, S. E. Hani, N. Naseri, A. Aghmadi, and K. E. Harouri, "Design and control of a small scale wind turbine emulator with a DC motor," in *2018 6th International Renewable and Sustainable Energy Conference (IRSEC)*. IEEE, Dec. 2018.

[5] H. Boudjemai, S. A. E. M. Ardjoun, H. Chafouk, M. Denaï, A. Alkuhayli, U. Khaled, and M. M. Mahmoud, "Experimental analysis of a new low power wind turbine emulator using a dc machine and advanced method for maximum wind power capture," *IEEE Access*, vol. 11, pp. 92 225–92 241, 2023.

[6] D. H. Wollz, S. A. O. da Silva, and L. P. Sampaio, "Real-time monitoring of an electronic wind turbine emulator based on the dynamic pmsg model using a graphical interface," *Renewable Energy*, vol. 155, pp. 296–308, Aug. 2020.

[7] Q.-C. Zhong and G. Weiss, "Synchronverters: Inverters that mimic synchronous generators," *IEEE Transactions on Industrial Electronics*, vol. 58, no. 4, pp. 1259–1267, Apr. 2011.

[8] Q.-C. Zhong, Y. Wang, Y. Dong, B. Ren, and M. Amin, "Go real: Power electronics from simulations to experiments in hours: Versatile experimental tool for next generation engineers," *IEEE Power Electronics Magazine*, vol. 7, no. 3, pp. 52–61, Sep. 2020.

[9] Q.-C. Zhong and W.-L. Ming, "A θ-converter that reduces common mode currents, output voltage ripples, and total capacitance required," *IEEE Transactions on Power Electronics*, vol. 31, no. 12, pp. 8435–8447, Dec. 2016.

[10] Q.-C. Zhong, W.-L. Ming, and Y. Zeng, "Self-synchronized universal droop controller," *IEEE Access*, vol. 4, pp. 7145–7153, Oct. 2016.

[11] Q.-C. Zhong and Z. Lyu, "Droop-controlled rectifiers that continuously take part in grid regulation," *IEEE Transactions on Industrial Electronics*, vol. 66, no. 8, pp. 6516–6526, Aug. 2019.

[12] H. Li and Z. Chen, "Overview of different wind generator systems and their comparisons," *IET Renewable Power Generation*, vol. 2, no. 2, pp. 123–138, Jun. 2008.

[13] T. Sun, Z. Chen, and F. Blaabjerg, "Voltage recovery of grid-connected wind turbines after a short-circuit fault," in *IECON03. 29th Annual Conference of the IEEE Industrial Electronics Society*, 2003.